System (16) was analyzed in [23] using the two-timing method (see e.g. [39], Section 7.6), aiming at finding periodic solutions and focusing on plots of the squared amplitude of the second cell, $|z_2|^2$, versus σ at selected representative values of μ. Here, we adopt a different approach by switching to a co-rotating frame and reducing the system, thereby eliminating the parameter λ and redefining the parameters μ and σ. This allows us to present a complete phase diagram in the (σ, μ)-plane in Fig. 10 and show that system (16) admits two types of attractors: stable limit cycles and invariant tori.

Let $\mu > 0$. We assume that the first oscillator is at its periodic attractor, i.e.,

$$z_1(t) = \sqrt{\mu} e^{\omega t i}. \tag{17}$$

Then we seek a solution for the second oscillator of the form

$$z_2(t) = u(t) e^{\omega t i} \equiv \left(u_R(t) + i u_I(t)\right) e^{\omega t i}, \tag{18}$$

where $u(t)$ is a complex-valued function that needs to be found, and u_R and u_I are its real and complex parts, respectively. Plugging Eqs. (17) and (18) into Eq. (16) and canceling the term $e^{\omega t i}$, we obtain the following equation for u:

$$\dot{u} = (\mu + i\sigma)u - |u|^2 u - \lambda\sqrt{\mu}. \tag{19}$$

4.1.1 Reducing the number of parameters

We aim to investigate the structure and stability of equilibria of Eq. (19) at all $\mu > 0$, $\sigma \in \mathbb{R}$, and $\lambda > 0$. Making $\lambda < 0$ has the same effect as multiplying u by the factor of $e^{i\pi/2}$. The equilibria of Eq. (19) correspond to periodic attractors of system (16). We aim to reduce the number of parameters from three to two. First, we normalize u by introducing $v := u/\sqrt{\mu}$. Then $|v| > 1$ means that the amplitude of z_2 is larger than that of z_1, and the other way around if $|v| < 1$. Next, we rescale the time as $\tau = \lambda t$. Then $\frac{d}{dt} = \lambda \frac{d}{d\tau}$. Finally, we divide the resulting ODE for v by λ and introduce $\tilde{\mu} := \mu/\lambda$ and $\tilde{\sigma} = \sigma/\lambda$. In summary, the reduction setup is

$$u = v\sqrt{\mu}, \quad \tau = \lambda t, \quad \tilde{\mu} = \frac{\mu}{\lambda}, \quad \tilde{\sigma} = \frac{\sigma}{\lambda}. \tag{20}$$

The resulting ODE for v has only two parameters, $\tilde{\mu}$ and $\tilde{\sigma}$:

$$\dot{v} = \tilde{\mu}(v - |v|^2 v) + i\tilde{\sigma} v - 1. \tag{21}$$

The corresponding system for the real and complex parts of v, $v = v_R + i v_I$, is:

$$\begin{aligned} \dot{v}_R &= \tilde{\mu}(1 - |v|^2) v_R - \tilde{\sigma} v_I - 1, \\ \dot{v}_I &= \tilde{\mu}(1 - |v|^2) v_I + \tilde{\sigma} v_R. \end{aligned} \tag{22}$$

4.1.2 Periodic solutions and their stability

We are primarily interested in phase-locked attractors of ODE (16), which correspond to equilibria of Eq. (21). Thus, we seek the roots of the system of algebraic equations

$$\begin{aligned} \tilde{\mu}(1 - |v|^2) v_R - \tilde{\sigma} v_I &= 1, \\ \tilde{\mu}(1 - |v|^2) v_I + \tilde{\sigma} v_R &= 0. \end{aligned} \tag{23}$$

Squaring the left-and right-hand sides of each equation in Eq. (23), adding them together, we find that the level sets of $|v|^2$ are semi-ellipses in the $(\tilde{\sigma}, \tilde{\mu})$-plane:

$$|v|^2 \tilde{\sigma}^2 + |v|^2 (1 - |v|^2)^2 \tilde{\mu}^2 = 1, \quad \tilde{\mu} > 0. \tag{24}$$

These semi-ellipses, shown in Fig. 10, are centered at the origin and have the semiaxes $r_{\tilde{\sigma}} = |v|^{-1}$ and $r_{\tilde{\mu}} = |v|^{-1} |1 - |v|^2|^{-1}$. If $|v|^2 > 2$, $r_{\tilde{\sigma}}$ is the major semiaxis, while if $|v|^2 < 2$, this is the other way

around. If $|v|^2 = 1$, the ellipse degenerates into two lines, $\tilde{\sigma} = \pm 1$. If $|v|^2 \in (0,1)$, the semi-ellipses fill out the exterior of the region bounded by $\tilde{\sigma} = 0$, the dark green dash-dotted curve in Fig. 10 defined by Eq. (31), and the lines $|\tilde{\sigma}| = \pm 1$. As $|v|^2$ increases from 0 to $\frac{1}{3}$, the semi-ellipses, plotted with gray dashed lines in Fig. 10, shrink to the semi-ellipse passing through $(0, \frac{3\sqrt{3}}{2})$. As $|v|^2$ further increases from $\frac{1}{3}$ to 1, the semi-ellipses, plotted with solid or dashed lines of grey shades, if $|v|^2 \in (\frac{1}{3}, \frac{1}{2})$, or red, brown and dark yellow shades, if $|v|^2 \in (\frac{1}{2}, 1)$, become thinner and taller, finally degenerating to the lines $\tilde{\sigma} = \pm 1$ as $|v|^2 \to 1$. If $|v|^2 > 1$, the semi-ellipses, plotted with blue and green solid lines, foliate the strip $|\tilde{\sigma}| < 1$ and shrink to a point around the origin as $|v|^2 \to \infty$. Throughout the rest of this paper, we will omit "semi-" for brevity and refer to the semi-ellipses as "ellipses".

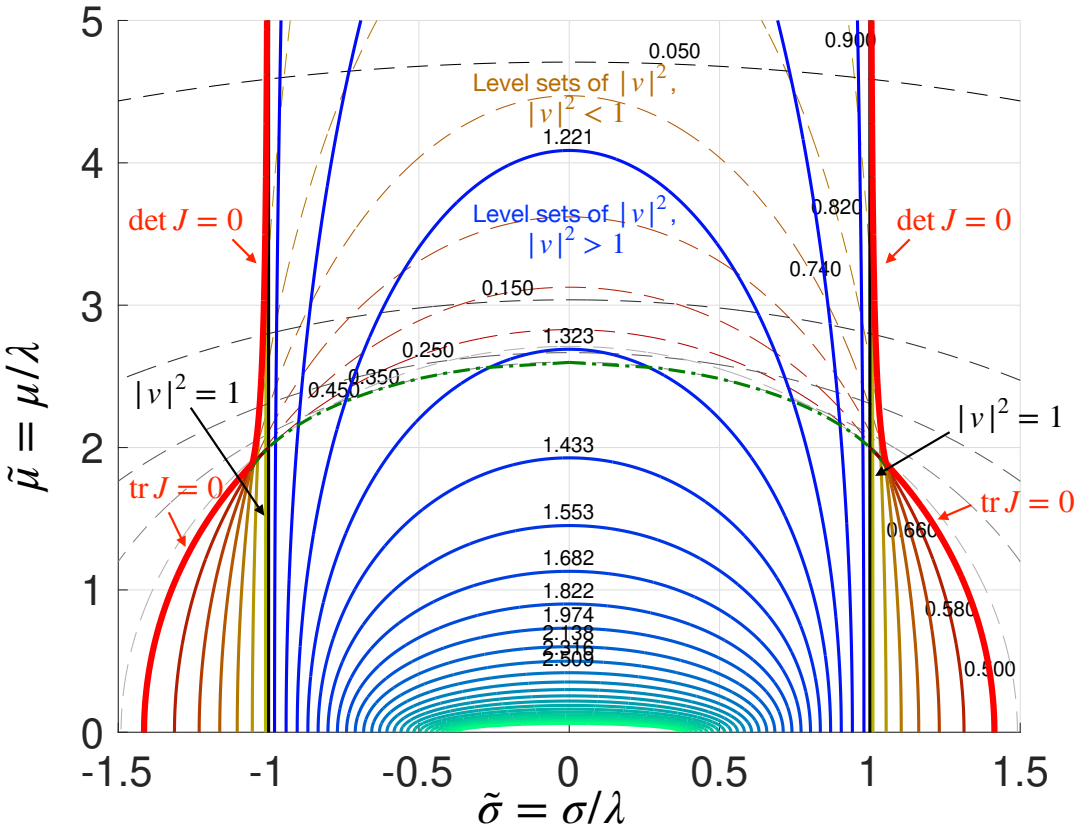

Figure 10: The phase diagram for system (16) with the inhomogeneity in the natural frequency in the parameter space $(\tilde{\sigma} = \sigma/\lambda, \tilde{\mu} = \mu/\lambda)$. The thick red curves belong to the boundary of the region where an asymptotically stable periodic solution to ODE (16) exists, i.e., the Stuart-Landau feedforward network with inhomogeneity in frequency is phase locked. A part of this thick red curves belong to the ellipse (29) corresponding to $\operatorname{tr} J(|v|^2) = 0$, i.e., $|v|^2 = \frac{1}{2}$. The other part belongs to the curve where $\det J = 0$ (Eq. (30)) plotted dash-dotted green. The medium-weight solid curves of blue and green shades depict the level sets of $|v|^2 > 1$ corresponding to asymptotically stable periodic solutions. The black vertical lines $\tilde{\sigma} = \pm 1$ correspond to stable periodic solutions with $|v|^2 = 1$. The medium-weight solid and thin dashed curves of red, brown and dark yellow shades correspond, respectively, to asymptotically stable and unstable periodic solutions with $\frac{1}{2} < |v|^2 < 1$. The dashed curves of grey tones depict ellipses with $0 < |v|^2 < \frac{1}{2}$. The black numbers next to the curves indicate the corresponding values of $|v|^2$.

The analysis of this family of ellipses allows us to discover dynamical properties of system (16). The stability of the equilibria of ODE (22) is determined by the signs of the determinant

and the trace of the Jacobian matrix of Eq. (22):

$$J(v_R, v_I) = \begin{bmatrix} \tilde{\mu}(1-|v|^2) - 2\tilde{\mu}v_R^2 & -\tilde{\sigma} - 2\tilde{\mu}v_I v_R \\ \tilde{\sigma} - 2\tilde{\mu}v_R v_I & \tilde{\mu}(1-|v|^2) - 2\tilde{\mu}v_I^2 \end{bmatrix}. \tag{25}$$

The conditions for the asymptotic stability are

$$\det J = \tilde{\mu}^2(1-|v|^2)(1-3|v|^2) + \tilde{\sigma}^2 > 0, \tag{26}$$

$$\operatorname{tr} J = 2\tilde{\mu}(1-2|v|^2) < 0. \tag{27}$$

The curve corresponding to $\operatorname{tr} J = 0$ is the ellipse with $|v|^2 = \frac{1}{2}$:

$$\frac{\tilde{\sigma}^2}{2} + \frac{\tilde{\mu}^2}{8} = 1. \tag{28}$$

It is depicted by the thick red solid line and the red dashed line in Fig. 10. The curve corresponding to $\det J = 0$ is plotted with the green dash-dotted line and the thick red solid line. A zoom-in of the kink of this curve is shown in Fig. 11. It is given parametrically by Eq. (31) below. Since the same pair $(\tilde{\sigma}, \tilde{\mu})$ admits up to three solutions, the task of finding the boundary of the region where an asymptotically stable equilibrium of Eq. (22) exists is nontrivial. The resulting boundary is highlighted with the thick red solid curve in Fig. 10. It turns out that the curve $\det J = 0$ also bounds the region where Eq. (22) has three equilibria. The ellipses with $|v|^2 \in (\frac{1}{3}, 1)$ touch the curve $\det J = 0$, rather than cross it, and the stability of the corresponding equilibria of Eq. (22) along each such ellipse changes at these tangent points. The structure and stability of the equilibria of Eq. (22) is summarized in Proposition 1.

Proposition 1. *1. Let $|\tilde{\sigma}| \le 1$. Then ODE (22) has a unique equilibrium with $|v| \ge 1$ at all $\tilde{\mu} > 0$, and this equilibrium is asymptotically stable.*

2. If $\tilde{\sigma} = 0$, the asymptotically stable equilibrium solution to ODE (22) is real and blows up as $|v| \approx \tilde{\mu}^{-1/3}$ as $\tilde{\mu} \to 0$.

3. The region in the $(\tilde{\sigma}, \tilde{\mu})$-space where an asymptotically stable equilibrium of ODE (22) exists is bounded by the arcs of the ellipse

$$\frac{\tilde{\mu}^2}{8} + \frac{\tilde{\sigma}^2}{2} = 1, \quad \tilde{\mu} \le \frac{4}{\sqrt{5}}|\tilde{\sigma}|, \tag{29}$$

and the curves defined implicitly as:

$$|v|^2 \in \left[\frac{3}{4}, 1\right), \quad \tilde{\sigma} = \pm\sqrt{\frac{3|v|^2-1}{2|v|^4}}, \quad \tilde{\mu} = \frac{1}{|v|^2\sqrt{2(1-|v|^2)}}, \tag{30}$$

The amplitude squared, $|v|^2$, of the asymptotically stable equilibrium solution ranges from $\frac{1}{2}$ to $+\infty$.

4. Three equilibria of ODE (22) exist in the region above the concatenation of the parametric curve

$$|v|^2 \in \left[\frac{1}{3}, 1\right), \quad \tilde{\sigma} = \sqrt{\frac{3|v|^2-1}{2|v|^4}}, \quad \tilde{\mu} = \frac{1}{|v|^2\sqrt{2(1-|v|^2)}} \tag{31}$$

and its reflection with respect to the $\tilde{\mu}$-axis. This curve starts at $(0, \frac{3\sqrt{3}}{2})$ at $|v|^2 = \frac{1}{3}$, has a singularity at $|v|^2 = \frac{2}{3}$, where $(\tilde{\sigma}, \tilde{\mu}) = (\frac{3}{2\sqrt{2}}, \frac{3\sqrt{3}}{2\sqrt{2}})$, associated with $\frac{d\tilde{\sigma}}{d|v|^2}(\frac{2}{3}) = 0$, and approaches the vertical asymptote $|v|^2 = 1$ from the right as $|v|^2 \to 1$.

The region with three equilibria is divided into three subregions by the ellipse $\frac{\tilde{\mu}^2}{8} + \frac{\tilde{\sigma}^2}{2} = 1$. Two asymptotically stable equilibria exist in the two subregions lying inside this ellipse and above the curve (31). Only one asymptotically stable equilibrium exists in the subregion outside the ellipse and above the curve (31).